Research Training Course in Detector Technology for Particle Physics

A Study of Semiconductor Diodes

Characterization of Common Diodes and Use as Detectors

Mikael Mårtensson

Uppsala University, mikael.martensson@physics.uu.se

December 10, 2015

Contents

1 Theory **1**
- 1.1 The pn semiconductor junction . . . 1
- 1.2 Depletion voltage of p^+n, n^+p, and p^+nn^+ diodes . . . 1
- 1.3 The Schottky interface . . . 2

2 Simulation of the pn diode **2**
- 2.1 An unbiased pn junction in equilibrium . . . 2
- 2.2 I-V curve for a p^+nn^+ diode . . . 3

3 Simulation of the Schottky diode **5**
- 3.1 Schottky interface in equilibrium . . . 5
- 3.2 Current-Voltage curve for a reverse biased Schottky diode . . . 6

4 Using the silicon diode as a detector **7**
- 4.1 Characterisation of the pre-amplifier . . . 8
- 4.2 Noise measurement of the spectroscopy amplifier . . . 9
- 4.3 Calibration spectrum and three point gain for the full setup . . . 9
- 4.4 Measurement of spectrum of ^{137}Cs and ^{241}Am . . . 10

5 Comparison clean room measurement of a p^+n diode sensor with simulations. **11**

References **13**

1 Theory

1.1 The pn semiconductor junction

The built in potential in a pn junction is given by

$$\Psi_0 = \frac{k_\mathrm{B} T}{q} \ln\left(\frac{N_\mathrm{A} N_\mathrm{D}}{n_\mathrm{i}^2}\right) , \tag{1}$$

where k_B is Boltzmann's constant, T is the temperature, q is the electron charge, N_A is the acceptor concentration, N_B is the donor concentration, and n_i is the intrinsic charge carrier concentration. The intrinsic charge carrier concentration at 300 K is $1.5 \times 10^{10}\,\mathrm{cm}^{-3}$ for Silicon (Si) and $2.5 \times 10^{13}\,\mathrm{cm}^{-3}$ for Germanium (Ge). Its temperature dependence is given by [1, eq. 10.1]:

$$n_\mathrm{i} = A T^{3/2} \exp\left(\frac{-E_\mathrm{g}}{2 k_\mathrm{B} T}\right) , \tag{2}$$

where A is a constant and E_g is the energy gap at 0 K.

The width of the depletion zone for a non-biased pn junction is [1, eq. 10.20]:

$$d = \sqrt{\frac{2\varepsilon_0 \varepsilon_\mathrm{r} \Psi_0}{q} \frac{(N_\mathrm{A} + N_\mathrm{D})}{N_\mathrm{A} N_\mathrm{D}}} , \tag{3}$$

where ε_0 is the dielectric constant (i.e. vacuum permittivity) and ε_r is the relative permittivity.

The maximum magnitude of the electric field occurs at the boundary between the p-doped and n-doped regions and is approximately given by [2, e.q. 11.21]:

$$E_\mathrm{max} \approx \frac{2\Psi_0}{d} . \tag{4}$$

1.2 Depletion voltage of $\mathrm{p^+n}$, $\mathrm{n^+p}$, and $\mathrm{p^+nn^+}$ diodes

For a lightly doped (n) donor bulk with a highly doped shallow acceptor ($\mathrm{p^+}$) implant the electric field in the shallow implant is very close to zero due to the abundance of available charge carriers. If a high enough reverse voltage is applied, the lightly doped bulk will be completely depleted, which means that the full voltage drops over the n-doped bulk and the depletion voltage is found by substituting $\Psi_0 \to \Psi_0 + V_\mathrm{d}$, putting $d = W_\mathrm{D}$, and taking the limit $N_\mathrm{A} \gg N_\mathrm{D}$ of equation 3:

$$V_\mathrm{d} = \frac{q W_\mathrm{D}^2 N_\mathrm{D}}{\varepsilon_0 \varepsilon_\mathrm{r}} \left(1 + \frac{N_\mathrm{D}}{N_\mathrm{A}}\right) - \Psi_0 . \tag{5}$$

The same is also valid for a $\mathrm{p^+n}$ diode by changing indices A↔D.

A $\mathrm{p^+nn^+}$ diode with width W, where $\mathrm{p^+}$ and $\mathrm{n^+}$ has the same dopant level, is identical to connecting a $\mathrm{p^+n}$ diode with width $W/2$ with a $\mathrm{nn^+}$ diode with width $W/2$. The depletion voltage is then:

$$V_{\mathrm{d}} = \frac{q(\frac{W}{2})^2 N}{\varepsilon_0 \varepsilon_{\mathrm{r}}} \left(1 + \frac{N}{N_+}\right) - \Psi_0 \tag{6}$$

where W is the width and N is the dopant concentration of the low-doped region (n), and N_+ is the dopant concentration of the highly doped regions (n^+ and p^+).

1.3 The Schottky interface

The Schottky diode is a simple metal-semiconductor contact. According to the Schottky-Mott model, the Schottky potential barrier is given by [3]:

$$\Phi_{\mathrm{B}} = \Phi_{\mathrm{m}} - \chi/q \ , \tag{7}$$

where Φ_{m} is the *work function* of the metal and χ is the *electron affinity* of the semiconductor.

The depletion depth can be derived from equation 3 by thinking of a metal as a very highly doped semiconductor, such that for example $N_{\mathrm{A}} \gg N_{\mathrm{D}}$. The equation then reduces to:

$$d = \sqrt{\frac{2\varepsilon_0 \varepsilon_{\mathrm{r}} \Phi_{\mathrm{B}}}{qN}} \ . \tag{8}$$

where N is the dopant concentration of the bulk.

2 Simulation of the pn diode

2.1 An unbiased pn junction in equilibrium

Here, a simulation of a small non-biased pn-diode in equilibrium is performed. The simulation model consists of a $3 \times 3\,\mu\mathrm{m}$ bulk of either a Si or Ge. Half the bulk is implanted with a donor (n-type dopant) and the other half with an acceptor (p-type dopant). Both region have a uniform dopant concentrations. The simulation's "doping scale" parameter was set to $1 \times 10^{16}\,\mathrm{cm}^{-3}$.

Several combinations of temperature, dopant concentration, and bulk material was simulated. Figure 1 shows the results. It shows the electron density, the hole density, the potential, and the electric field probed along the line in the middle of the diode. Several thing can be observed:

- A **higher temperature** slightly increases the minority carrier concentration, probably due to thermal excitation, which results in a slightly lower built in potential difference and slightly lower maximum electric field amplitude.
- A **higher doping** concentration lowers the electrons (hole) concentration in the p-region (n-region) which results in a larger potential difference. The electron-hole transition also becomes sharper, which causes the potential transition to be

			Ψ_0 (V)		d (µm)		$E_{\max}$ (V µm^{-1})	
T (K)	N_x (cm^{-3})	Si/Ge	Theory	Sim.	Theory	Sim.	Theory	Sim.
284	1×10^{16}	Si	0.73	0.74	0.44	0.49	3.33	3.16
300	1×10^{16}	Si	0.69	0.71	0.43	0.48	3.26	3.08
316	1×10^{16}	Si	0.66	0.68	0.42	0.47	3.19	3.00
300	1×10^{15}	Si	0.57	0.59	1.22	1.26	0.94	0.90
300	1×10^{17}	Si	0.81	0.83	0.15	0.15	11.16	10.31
300	1×10^{16}	Ge	0.23	0.32	0.28	0.41	1.60	1.64

Table 1: Comparison of theory and simulation for a pn junction. The simulated depletion depth was taken to be the distance between the points where the electric field drops below 10% of its maximum.

sharper, decreases the depletion depth, and increased the magnitude of the electric field.

- When **changing the bulk material** from **Si** to **Ge**, the minority charge carrier concentration increases with about 3 orders of magnitude. This is due to the higher intrinsic charge carrier concentration of Ge (2.5×10^{13} cm^{-3} compared to 1.5×10^{10} cm^{-3} for Si). This makes the potential difference for the Ge diode lower, the depletion depth smaller, and the maximum electric field lower compared to that of the Si.

Table 1 compares the simulation results to calculations using eqs. (1) to (4). The simulated depletion depth was taken to be the distance between the points where the electric field drops below 10 % of its maximum. For silicon the results agree very well. However, for germanium the built in potential and the depletion depth differs significantly. Why this is the case is unknown.

Might see the same effect in Si at much elevated temperature

2.2 I-V curve for a p$^+$nn$^+$ diode

The p$^+$nn$^+$ diode simulation model consists of 100×50 µm lightly n-doped Si bulk with a donor concentration of 1×10^{13} cm^{-3}. The first 3 µm of each short end is highly doped with n$^+$-type on one side and p$^+$-type on the other, both with dopant concentrations of 1×10^{18} cm^{-3}. A Gaussian doping distribution with characteristic length of 1 µm was used. The anode and cathode contacts are 3 µm wide and connected to the edge of the n$^+$-region and p$^+$-doped region respectively. A reverse bias direct current (DC) sweep between 0 V and 100 V was performed. The doping scale simulation parameter was set to 1×10^{16} cm^{-3}.

Reverse bias Figure 2a and 2b shows the simulated I-V curve for reverse biased pn diode for Si and Ge respectively. The depletion voltage for silicon appears to be close to 65 V. The smooth I-V curve of germanium makes it harder to tell its depletion voltage,

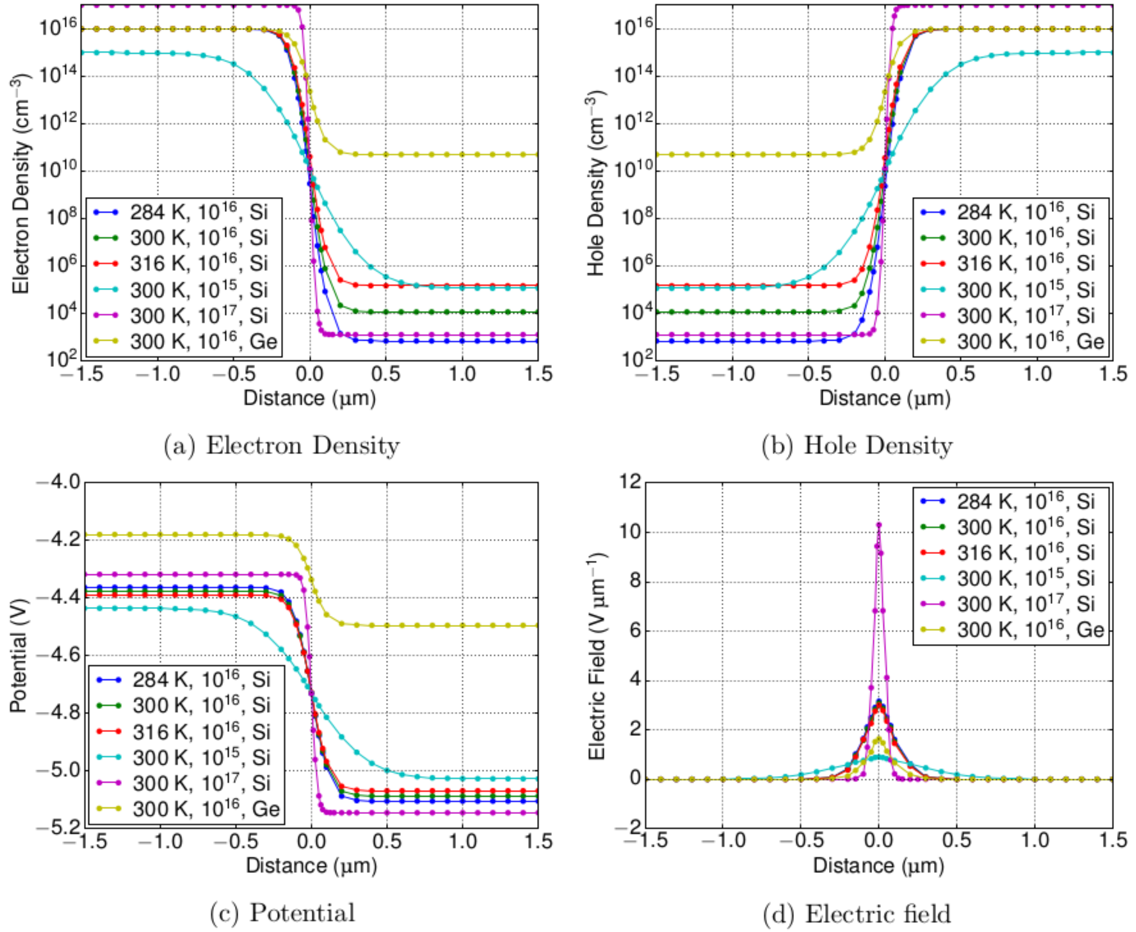

(a) Electron Density

(b) Hole Density

(c) Potential

(d) Electric field

Figure 1: Simulation of a pn junction. The temperature of the substrate, the doping level in cm^{-3}, and the substrate type is seen in the legend. The junction is located at 0 µm.

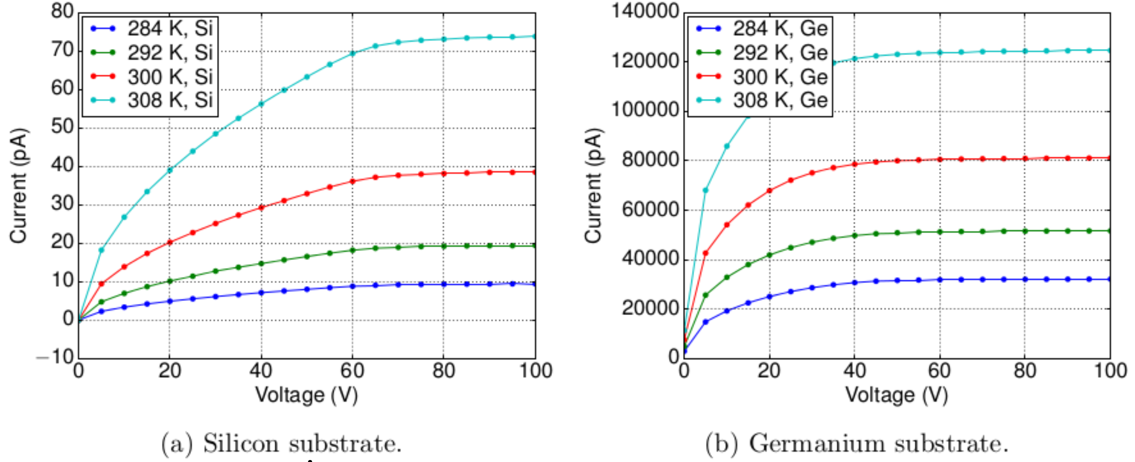

(a) Silicon substrate.

(b) Germanium substrate.

Figure 2: Current-Voltage (I-V) curve for a reversed biased PN diode.

but it appears to be near to 50 V. It is also noteworthy that the leakage current roughly double each 8 K for silicon and increases with around 50 % for germanium.

The depletion voltage for the two cases in figure 2 was also calculated using equation 6 with width $W = 100 - 2 \times 3\,\mu\text{m} = 96\,\mu\text{m}$. It was found to be $V_\text{d} = 66.5\,\text{V}$ for silicon, and $V_\text{d} = 49.6\,\text{V}$ for germanium; a surprisingly good agreement.

Forward bias Figure 3 shows the simulated I-V curve for a forward biased diode. Figure 3a shows the forward breakdown region with the characteristic exponential I-V shape. The germanium diode breaks down earlier than the silicon. This is in good agreement with literature, which states a typical forward break down voltage of 0.3 V for germanium diodes and 0.7 V for silicon.

Figure 3a shows the I-V curve for larger voltages. This shows the behavior after the exponential break down at lower voltages, and the current limiting property at larger voltages.

3 Simulation of the Schottky diode

3.1 Schottky interface in equilibrium

The Schottky diode interface consists of a $2 \times 3\,\mu\text{m}$ large p-doped region with a $1 \times 3\,\mu\text{m}$ Schottky contact, i.e. metal contact. The interface is at $y = 0\,\mu\text{m}$. The doping scale simulation parameter was set to $1 \times 10^{18}\,\text{cm}^{-3}$.

Figure 4 shows the electron density, hole density, potential, and electric field for the Schottky diode. Table 2 shows the built in potential, depletion depth, and maximum electric field. The result is heavily dependent on the work function of the metal. However, if the result is compared with that of the pn diode in section 2 for similar parameters, e.g. silicon bulk with a temperature of 300 K and dopant concentration of $1 \times 10^{15}\,\text{cm}^{-3}$, it

What value was the work function given

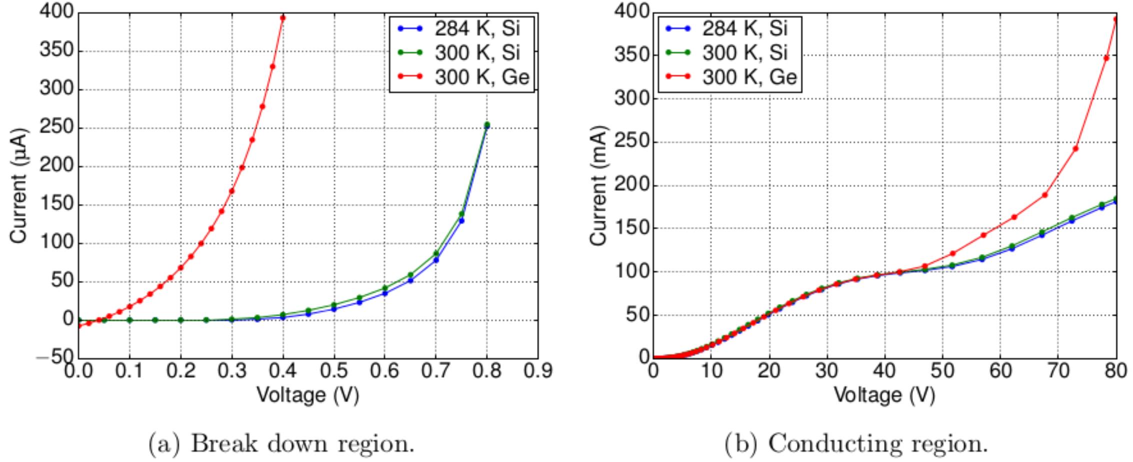

(a) Break down region.

(b) Conducting region.

Figure 3: Current-Voltage (I-V) curve for a forward biased PN diode.

				Φ_B (mV)		d (µm)		E_{max} (mV µm^{-1})	
T (K)	N_x (cm^{-3})	Φ_m (V)	Si/Ge	Theory	Sim.	Theory	Sim.	Theory	Sim.
300	1×10^{15}	4.2	Si	150	8.56	0.44	0.39	3.33	61.79
284	1×10^{15}	4.2	Si	150	9.49	0.43	0.38	3.26	69.77
300	2×10^{15}	4.2	Si	150	0.46	0.42	0.29	3.19	5.21
300	1×10^{15}	4.4	Si	350	0.53	1.22	0.38	0.94	39.21
300	1×10^{15}	4.2	Ge	200	1.00	0.15	0.42	11.16	0.42

Table 2: Comparison of theory and simulation for a Schottky diode. The simulated depletion depth was taken to be the distance between the points where the electric field drops below 10% of its maximum.

is clear that the built in potential is two orders of magnitude lower, the depletion depth is about one third, and the maximum electric field is one order of magnitude lower.

The theoretical calculations of the built in potential, depletion depth, and maximum electric field in table 2 were made using eqs. (4), (7) and (8), where Ψ_0 was substituted for Φ_B in the last equation. The simulations and calculations differs significantly. This is because the Schottky-Mott model of the built in potential is very rough. It is based on the notion of contacting metal and semiconductor in vacuum. In reality the potential is affected by chemical bonding and the existence of surface states.

Correct, a reason why surface barrier diodes are not very popular.

3.2 Current-Voltage curve for a reverse biased Schottky diode

The Schottky diode simulation model has a 50×97 µm n-doped Si bulk with an donor concentration of 1×10^{15} cm^{-3} and a 3 µm Schottky contact on the short side. The lattice temperature is 300 K. The doping scale simulation parameter was set to 1×10^{18} cm^{-3}.

The I-V curve for the reverse biased Schottky diode is shown in figure 5. The depletion

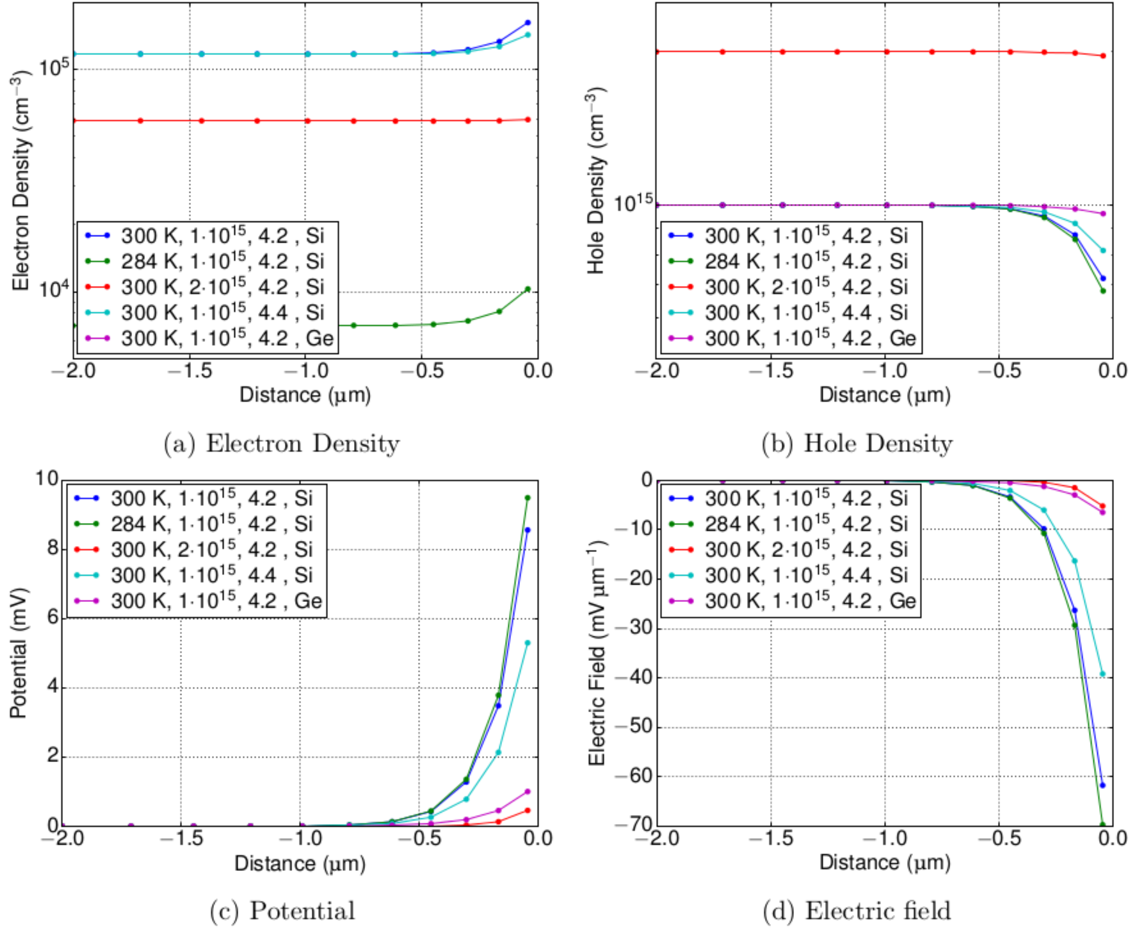

(a) Electron Density

(b) Hole Density

(c) Potential

(d) Electric field

Figure 4: Simulation of a Schottky diode metal-semiconductor interface. The legend shows the lattice temperature, the acceptor doping concentration, and the Schottky contact work function.

voltage seems to be around 20 V which is about one-third of the pn diode in section 2.2. The reverse current of the Schottky diode is much higher than the pn diode: mA compared with pA. However, a direct comparison of the depletion voltage is unfair since the bulk doping level is different for the Schottky and pn diode. It was not possible to make the Schottky diode deplete using the same bulk as for the pn diode.

4 Using the silicon diode as a detector

A silicon diode sensor is used with a standard amplifier chain and Multi-Component Analyser (MCA) to measure the spectrum of ^{137}Cs and ^{241}Am. The amplifier chain consisting of a charge-sensitive pre-amplifier and a Spectroscopy Amplifier (SA) (also known as a pulse shaper). The setup is seen in figure 6. The pre-amplifier has a test

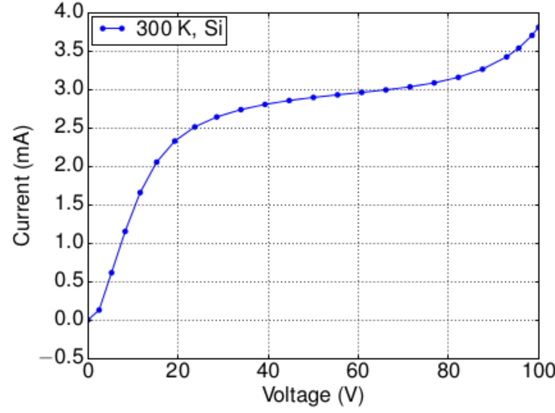

Rather high current.
What work function used?
Possibly forward bias?

Figure 5: Current-Voltage (I-V) curve for the Schottky diode.

capacitor C_{test} and the possibility to apply a capacitive load C_{load}. The pre-amplifier and SA is characterized, and in the end spectra are acquired using the MCA.

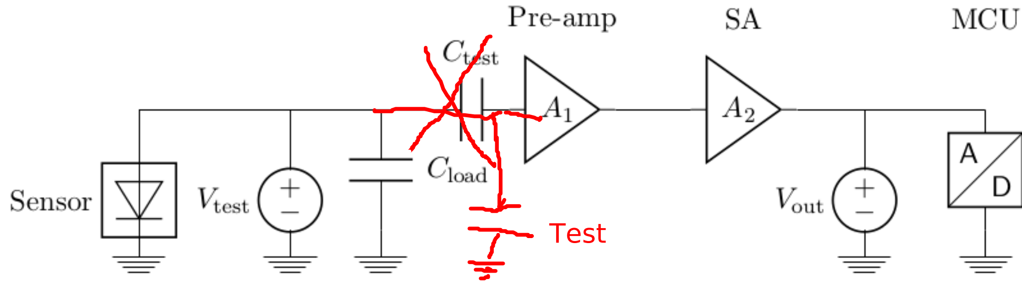

Figure 6: Silicon diode detector setup.

4.1 Characterization of the pre-amplifier

The charge-sensitive pre-amplifier is characterized by injecting charge through the test input capacitor. The charge stored on a capacitor is determined by:

$$Q = CV \tag{9}$$

where C is the capacitance and V is the voltage applied across the two terminals. In this case $C = C_{\text{test}} = 0.4\,\text{pF}$. So if the wanted charge injection is

$$Q = 25\,000\,e = \frac{25\,000\,e}{6.241 \times 10^{18}\,e\,\text{C}^{-1}} \approx 4.01 \times 10^{-15}\,\text{C}\ ,$$

the voltage that should be applied is:

$$V = Q/C_{\text{test}} \approx 10\,\text{mV}\ .$$

The gain was characterized by measuring the output amplitude and rise time of the pre-amplifier with an oscilloscope when applying a square-wave input of 10 mV with a frequency of 1 kHz for various load capacitances. The time and voltage scale of the oscilloscope was set to 20 ns/div and 20 mV/div. For the noise measurement, the calibration input was turned of and the oscilloscope set to 100 µs/div and 1 mV/div. Table 3 and figures 7a, 7b, and 7c shows the results.

C_{load} (pF)	Amplitude (mV)	Rise time (ns)	V_{rms} (µV)	FWHM(V_{rms}) (µV)
100	20.3	56.9	291	62
54	27.3	50.5	247	51
27	33.3	39.3	212	45
10	38.9	32.5	194	48
4.7	40.1	30.5	182	46
1	40.0	28.1	169	40
No load	-	-	184	44

Table 3: Characterization of the pre-amplifier as a function of load capacitance

The Equivalent Noise Charge (ENC) was calculated using equation 9 with $V = V_{\text{rms}}$ and $C = C_{\text{test}} = 0.4\,\text{pF}$. The result is shown in figure 7d. Also shown there is the noise measured after the shaper, which is described in section 4.2. A line was fitted to the ENC curve to extract the *pedestal noise* (noise at $C = 0$) and *noise slope*. They were determined to be $376 \pm 63\,e$ and $3.05 \pm 0.11\,e\,\text{pF}^{-1}$ respectively.

Not correct. ENC= V(rms)/V(signal) * Q -> ENC@1pf = 103

4.2 Noise measurement of the spectroscopy amplifier

The noise of the SA for two combinations of shaping time was measured with an oscilloscope for a load capacitance of 27 pF in the same way as for the pre-amplifier. The SA gain was set to 100. The result is included in figures 7a and 7d. As expected, the SA improves the noise performance significantly, and the longer shaping time performs better (although a too long shaping time would have problem with pile-up in a high rate environment).

Noise can be categorized in two main categories: noise that is *parallel* or *serial* to the input. The second kind is the hardest one to get rid of, since that is amplified just as if it is a signal. Serial noise is not amplified. The observation that the signal shaped by the SA has lower noise leads to the conclusion that parallel noise is a large contribution.

4.3 Calibration spectrum and three point gain for the full setup

The calibration spectrum for three setting of the SA and a 3-point gain calibration for one setting of the SA was performed with the full setup by applying calibration pulses V_{test} with $C_{\text{load}} = 27\,\text{pC}$ and measuring the output with the MCA. For the 3-point gain curve the SA was set to gain 500 and a shaping time of 16 µs. The result is seen in figure 8. A line was fitted to the 3-point gain curve. The test capacitance $C_{\text{test}} = 0.4\,\text{pC}$

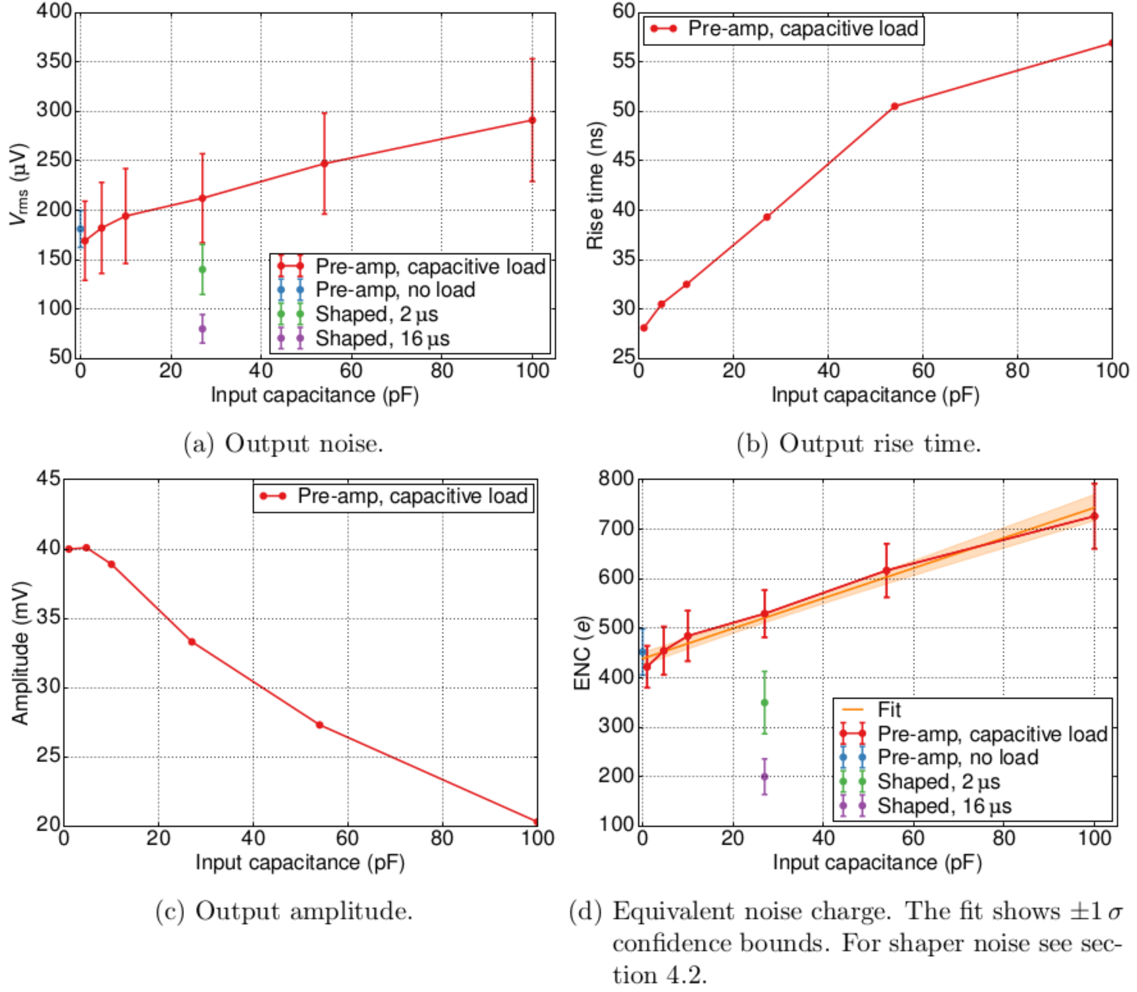

(a) Output noise.

(b) Output rise time.

(c) Output amplitude.

(d) Equivalent noise charge. The fit shows $\pm 1\,\sigma$ confidence bounds. For shaper noise see section 4.2.

With correct ENC calc the curve will be shifted down

Figure 7: Characteristics of the pre-amplifier as a function of load capacitance. Amplitude and rise time was measured for a fixed square-wave input of 10 mV at 1 kHz. Noise was measured without any input voltage. Error bars show $1\,\sigma$ errors calculated from FWHM as measured with an oscilloscope.

was used to convert from voltage to charge (equation 9). The offset was found to be 2.637×10^{-4} pC and the slope 1.860×10^{-6} pC ch^{-1}.

4.4 Measurement of spectrum of ^{137}Cs and ^{241}Am

The spectrum of ^{137}Cs and ^{241}Am was measured using the full setup with a 35 V reverse bias applied to the silicon diode sensor. Figure 9a and 9b shows the result. The calibration from the 3-point gain discussed in section 4.3 was applied to the Am spectrum and a fit consisting of a linear background and a Gaussian peak was fitted to extract the resolution. This is seen in figure 9c. The resolution was found to be

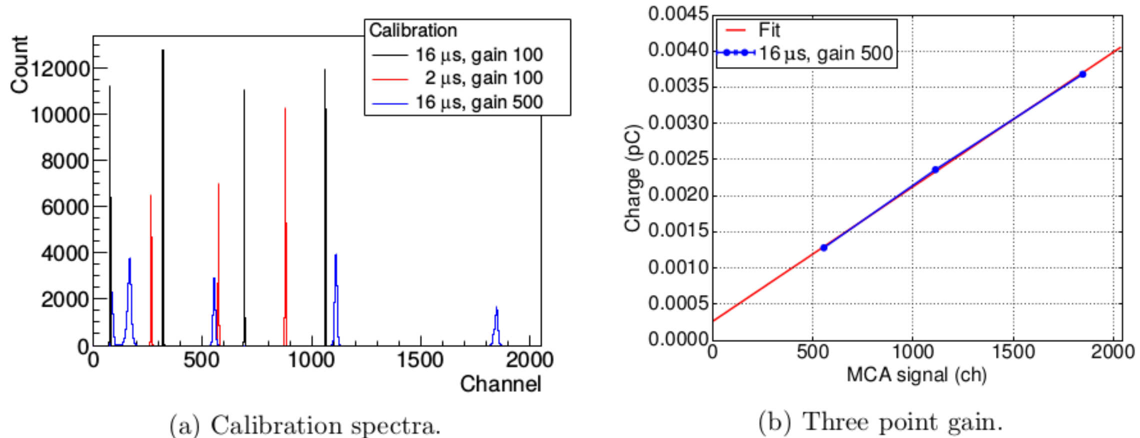

(a) Calibration spectra.

(b) Three point gain.

Figure 8: Calibration and 3-point gain for the full setup. The left-most line of the spectrum for gain 500 and shaping time 16 µs is noise.

$$\frac{\Delta Q}{Q} = \frac{2.27 \times 10^{-2}\,\mathrm{fC}}{3.30 \times 10^{-1}\,\mathrm{fC}} \approx 6.9\,\% \,.$$

The gamma peak of ^{241}Am is known to be at 59.5 keV and the energy required to create one charge carrier in silicon is 3.62 eV [2]. So the gamma is expected to deposit

$$\frac{59.5\,\mathrm{keV}}{3.62\,\mathrm{eV}} \times 1.6 \times 10^{-19}\,\mathrm{C} = 2.63\,\mathrm{fC} \,.$$

However, the peak is located at 0.330 fC, which is a only 12 % of the expected value. This shows that the 3-point calibration described in section 4.3 is wrong. Possible explanation include C_{test} being a factor $\sim 1/0.12 \approx 8$ larger, or that the oscilloscope was used with $\times 10$ attenuation. If the test capacitance is indeed higher, the ENC of figure 7d would scale linearly with the increased capacitance.

5 Comparison clean room measurement of a p$^+$n diode sensor with simulations

The pn diode consists of a 300 µm n-type bulk with donor concentration $1 \times 10^{12}\,\mathrm{cm}^{-3}$ with a 2 µm thick p-type implant with an acceptor concentration of $5 \times 10^{18}\,\mathrm{cm}^{-3}$ and 0.5 µm thick aluminum electrodes on both sides. The active area is 5×5 mm. For the simulation, the model was limited to a 50×5000 µm slice with periodic boundary conditions and the resulting leakage current scaled up by a factor 100. The doping scale simulation parameter was set to $5 \times 10^{18}\,\mathrm{cm}^{-3}$. The lattice temperature was set to 293 K (20 °C) which was the approximate temperature in the clean room.

The CV-curve and IV-curve of a real diode was measured in a clean room environment and a IV-scan was simulated. Figure 10 shows the IV-curve for the measurement and

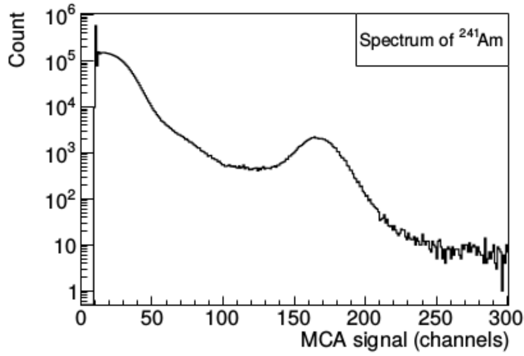

(a) Spectrum of ^{241}Am. Note the logarithmic scale.

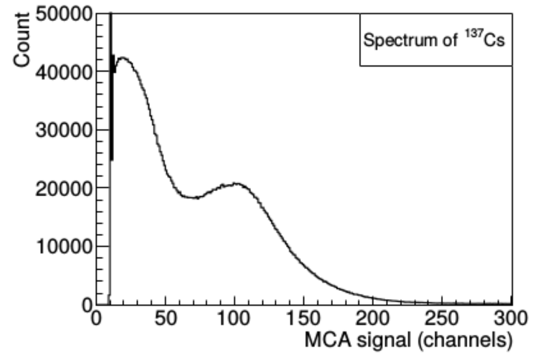

(b) Spectrum of ^{137}Cs.

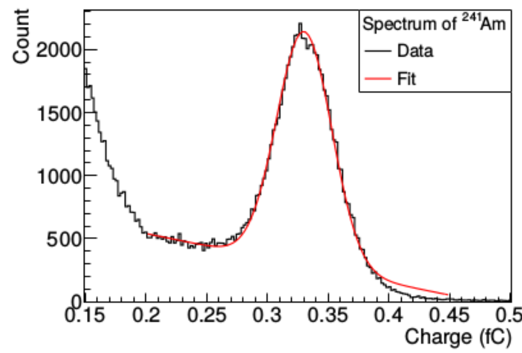

(c) Fit of a linear background and Gaussian to the ^{241}Am peak.

Figure 9: Calibration and 3-point gain for the full setup. The left-most line of the spectrum for gain 500 and shaping time 16 µs is noise.

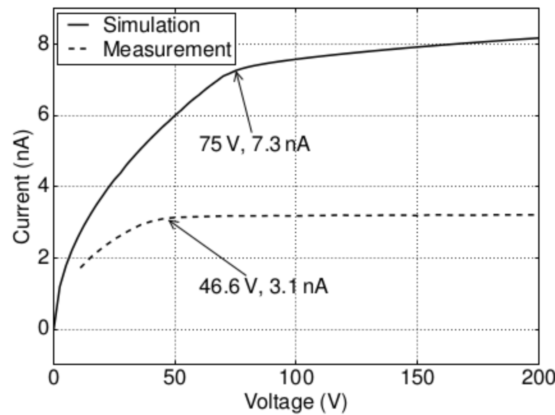

Figure 10: Comparison of IV-curves for a real diode and simulation.

the simulation. The depletion voltage of the real diode was determined to be 46.6 V by fitting two straight lines to the CV-curve (not shown here). The simulation shows a depletion voltage at approximately 75 V which is significantly higher than the real diode. The leakage current at full depletion is also a factor of 2 higher for the simulation. The reason for the big discrepancy is unknown, but possible reasons include using the wrong geometry and/or doping in the simulation, or imperfections in manufacturing the real diode.

Perhaps the given dopings were not correct?

References

[1] W. R. Leo. *Techniques for Nuclear and Particle Physics Experiments*. Springer-Verlag, 2 edition, 1994.

[2] Glenn. F. Knoll. *Radiation Detection and Measurement*. John Wiley & Sons, Inc., 4 edition, 2010.

[3] Richard Brenner. Lecture on semiconductor basics. Course in Detector Technology for Particle Physics, 2015.